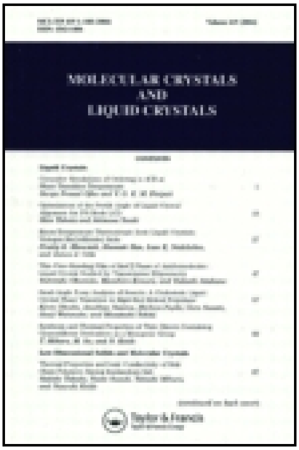

Molecular Crystals and Liquid Crystals Science and Technology. Section A. Molecular Crystals and Liquid Crystals

Publication details, including instructions for authors and subscription information:
http://www.tandfonline.com/loi/gmcl19

Electron Transfer in Supermolecules

Joshua Jortner [a] & M. Bixon [a]

[a] School of Chemistry, Tel Aviv University Ramat Aviv, Tel-Aviv, 69978, Israel

Version of record first published: 04 Oct 2006.

To cite this article: Joshua Jortner & M. Bixon (1993): Electron Transfer in Supermolecules, Molecular Crystals and Liquid Crystals Science and Technology. Section A. Molecular Crystals and Liquid Crystals, 234:1, 29-41

To link to this article: http://dx.doi.org/10.1080/10587259308042895

Mol. Cryst. Liq. Cryst. 1993, Vol. 234, pp. 29–41
Reprints available directly from the publisher
Photocopying permitted by license only

Printed in the United States of America

ELECTRON TRANSFER IN SUPERMOLECULES

JOSHUA JORTNER AND M. BIXON
School of Chemistry, Tel Aviv University
Ramat Aviv, Tel-Aviv 69978, Israel

Abstract. Energy storage and disposal by electron transfer in molecular and supermolecular systems may provide a conceptual and technical basis for the construction of molecular electronic devices, e.g., molecular wires and switches. We consider structural, intramolecular, medium energetic and medium dynamic control of electron transfer in synthetic and neutral supermolecules. Optimization principles are formulated for ultrafast, highly efficient and stable charge separation.

1. INTRODUCTION

The outstanding goal of molecular electronics pertains to the perspective utilization of miniaturization on the molecular level to accomplish a huge density of devices, e.g., molecular wires, switches, transistors and memories. Necessary conditions for the utilization of such molecular electronic devices are high-efficiency (yield) and error-free operation. The microscopic mechanisms underlying the operation of such molecular systems fall into two major categories: (i) electronic and ionic transport in the ground electronic state, and (ii) excited-state relaxation. The latter processes are commonly triggered by optical excitations, encompassing a variety of intramolecular and intermolecular radiationless processes,[1] e.g., electronic-vibrational relaxation, vibrational energy redistribution, isomerization, proton transfer and electron transfer (ET). Energy storage and disposal via ET in molecular and supermolecular systems[2] is expected to provide a central conceptual and technical basis to the potential emergence of molecular electronics. ET in supermolecules falls into two general categories:

(1) Man-made synthetic supermolecules[3-6] consisting of an electron donor (D), and an electron acceptor (A), linked by a nonrigid or a rigid molecular bridge (B).

(2) Nature-made supermolecules such as the photosynthetic reaction centers (RC) of bacteria and plants,[7] where the primary process of the conversion of solar energy into chemical energy proceeds via a sequence of well organized, highly efficient, directional and specific ET processes between prosthetic groups embedded in the protein medium.

Photophysical and photobiological ET from an electronically excited donor proceeds via superexchange mediated or direct processes $DBA \xrightarrow{h\nu} D^{*}BA \xrightarrow{ET} D^{+}BA^{-}$ or $DA \xrightarrow{h\nu} D^{*}A \xrightarrow{ET} D^{+}A^{-}$. The control of ET in DBA or DA systems in solution,[2] in a solid,[2] in a protein[2,7] or within an "isolated" solvent-free supermolecule[8] can be accomplished by:

(1) Structural control. "Molecular engineering" of the D, A and B subunits determines the molecular energetics and the direct D-A or superexchange D-B-A electronic coupling.

(2) Intramolecular dynamic control of the nuclear equilibrium configurational changes (i.e., nuclear distortions) accompanying ET.[2]

(3) Medium control of "conventional" ET in a solvent or in a cluster. The function of the medium on the $DBA \rightarrow D^{+}BA^{-}$ ET is:[8] (i) The energetic stabilization of the ionic states. (ii) The coupling of the electronic states with the medium nuclear motion, which originates from short-range and long-range interactions in polar solvents, short-range interactions with C-H group dipoles in nonpolar hydrocarbons and with polar amino acid residues in proteins.

(4) Dynamic medium control of ET[9] involving: (i) The medium acting as a heat bath. The relaxation of the medium polar modes is often fast on the time scale of the electronic ET processes, which then constitute the rate determining step. (ii) Dynamic solvation effects of DBA or/and $D^{+}BA^{-}$ determine the ET dynamics when condition (i) is violated and solvent-controlled ET may be exhibited.

The structural, intramolecular, solvent and dynamic control of ET will allow for the formulation of an optimization principle allowing for the design of molecular systems where ET is: (a) Ultrafast (on the time scale of ~ 1 psec to ~ 100 fsec) overwhelming any energy waste processes. (b) Highly efficient, eliminating any backreactions. (c) Stable with respect to the predictable variation of molecular and medium properties. (d) Practically invariant with respect to temperature changes.

2. THEORETICAL FOUNDATIONS

Basic ET Theory

The nonadiabatic ET rate is given by[2-7,10] $k = (2\pi/\hbar)V^2F$, where V is the electronic coupling and F is the thermally averaged nuclear vibrational Franck-Condon factor. This microscopic description rests on the following description and conditions:

(A) ET is described as a radiationless transition.

(B) The applicability of the Born-Oppenheimer separability of electronic and nuclear motion, allowing for the description of the system in terms of diabatic potential surfaces (Fig. 1).

(C) The electronic coupling is sufficiently weak to warrant the description of the radiationless transition in the nonadiabatic limit.

(D) Insensitivity of microscopic ET rates to medium dynamics. This state of affairs is realized under one of the following conditions: (i) The common situation of fast medium vibrational dynamics, which allows for the separation of time scales with the microscopic ET rate constants constituting the rate determining step.[9] (ii) The microscopic ET rates weakly depend on the distribution in the initial D^*BA vibronic manifold.[11]

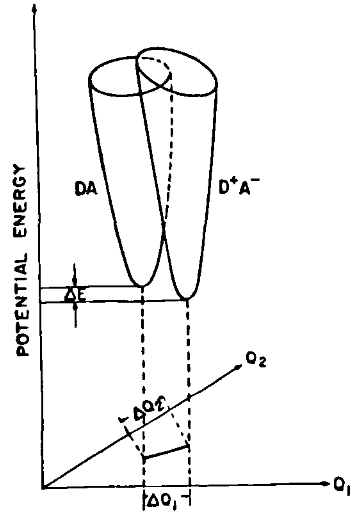

FIGURE 1 Diabatic nuclear potential energy surfaces for DA → D^+A^- ET. The nuclear coordinates incorporate the medium and the intramolecular coordinates. The displacements of the equilibrium configurations are marked as ΔQ_1, ΔQ_2.

Electronic Coupling

The electronic coupling in the DBA system $V = V_{DA} + V_{super}$ consists of a sum of a direct D-A exchange contribution $V_{DA} = \langle \phi^0_{DA} | \hat{H} | \phi^0_{D^+A^-} \rangle$ between the electronic states of DA and D^+A^-, and a superexchange[2,11] $V_{super} = V_{DB} V_{BA} / \delta E_B$, where δE_B is the vertical energy difference between the potential energy surfaces (PES) of DBA and D^+BA^-. For superexchange between closed shell D, B and A systems both direct and superexchange interactions require the evaluation of individual pair V_{DA}, V_{DB} or V_{BA} couplings, while for intramolecular superexchange in D-B-A supermolecules molecular calculations were utilized.[12] In both cases many-electron computations, transcedenting the naive one-electron picture, have to be invoked. The accumulated information concerning the distance dependence of both direct and superexchange interactions is that both interactions are expected to exhibit an exponential distance dependence[2-7,10]

$$V = a \exp(-\beta R_{DA}) \ , \tag{2.1}$$

where R_{DA} is the (either edge-to-edge or center-to-center) D-A distance. The distance dependence of intramolecular superexchange interactions in synthetic supermolecules and in the photosynthetic reaction center (Fig. 2) was inferred from the analysis of either ET rates or optical charge transfer spectra. The general trend confirms the exponential relation, Eq. (2.1), quantified by β, which is system specific. On the basis of these exponential relations one cannot infer, a priori, whether the electronic coupling is direct or superexchange mediated, and further theoretical input is required. Alluding to molecular electronics, the minimization of β will be desirable for molecular wires.

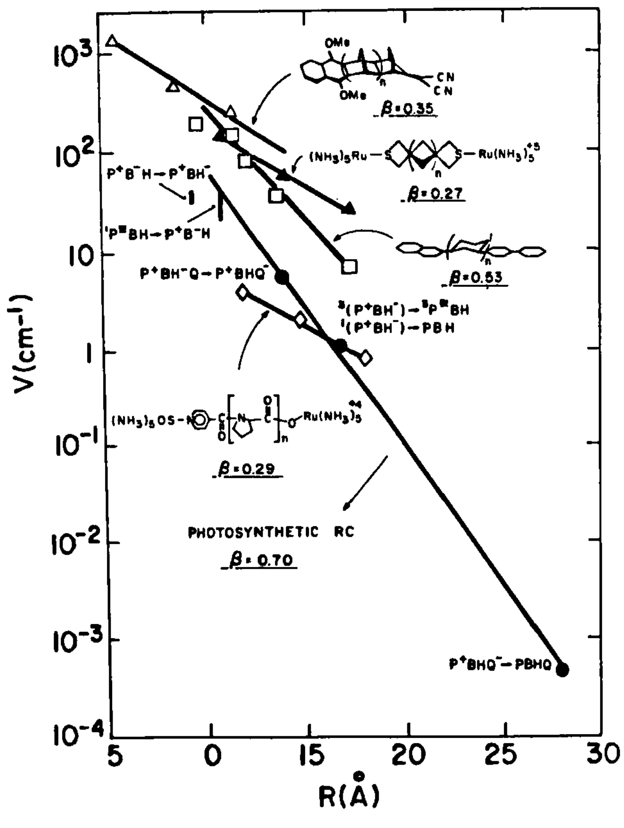

FIGURE 2 The distance dependence of V for synthetic supermolecules obtained from kinetic and spectroscopic data (references 3-6 and 12) and for the bacterial photosynthetic RC obtained from analysis of kinetic data (references 7, 9, 13, 14). The system specific β values (in Å^{-1}) are presented on the figure.

(2.C) Nuclear Franck-Condon Factors

The nuclear Franck-Condon factor F in Eq. (2.1) contains the thermal average of the overlap integrals between the initial and final vibrational states of the system, under the restriction of energy conservation. For two harmonic potential energy surfaces characterized by identical reduced masses $\{\mu_i\}$, frequencies $\{\omega_i\}$, normal modes $\{Q_i\}$ and nuclear displacement $\{\Delta Q_i\}$ of the equilibrium coordinates (Fig. 1), F takes the form of a Fourier transform[10]

$$F = (2\pi)^{-1} \exp(-G) \int_{-\infty}^{\infty} dt \exp(-i\Delta Et) \exp[G_+(t) + G_-(t)] \ , \qquad (2.2)$$

where ΔE is the energy gap, and

$$G_\pm(t) = \sum_i (\Delta_i^2/2) \begin{Bmatrix} \bar{v}_i+1 \\ v_i \end{Bmatrix} \exp(\pm i\omega_i t) \qquad (2.3)$$

$$G = G_+(0) + G_-(0) \qquad (2.4)$$

$$\bar{v}_i = [\exp(\hbar\omega_i/k_B T)-1]^{-1} \qquad (2.5)$$

$$\Delta_i = (\mu_i \omega_i/\hbar)^{1/2} \Delta Q_i \ . \qquad (2.6)$$

$\bar{v}_i$ denotes the thermal average and is the reduced displacement of the ith mode, while exp(-G) is the Debye-Weller factor. Eq. (2.2) was advanced for multiphonon optical transitions, for radiationless transitions in general and for ET in particular. Several equivalent forms of this expression were recently presented.

The vibrational modes incorporated in Eq. (2.2) include:

(i) Low-frequency medium modes, which are usually approximated by a single frequency ω_m with an effective Δ_m. "Intelligent guesses" for glasses result in $\omega_m \simeq 10\text{-}100\ \text{cm}^{-1}$. It seems that for a polar solvent a phonon picture is not applicable, while for a protein medium[13] $\omega_m \sim 100\ \text{cm}^{-1}$. The medium reorganization energy is $\lambda_m = S_m \hbar\omega_m$, where $S_m = \Delta_m^2/2$. For polar solvents $\lambda_m = 4000\text{-}8000\ \text{cm}^{-1}$,[2] while for the protein RC $\lambda_m \simeq 800\text{-}3000\ \text{cm}^{-1}$.[13]

(ii) Intramolecular modes in the range $\omega \simeq 100\text{-}3000\ \text{cm}^{-1}$. Often, but not exclusively, the medium modes can be approximated by a single molecular frequency $\omega_c \simeq 1500\ \text{cm}^{-1}$ and a dimensionless shift $S_c = \Delta_c^2/2 \simeq 1$.[13]

Energy gap laws constitute a major generalization of microscopic relaxation phenomena, which originate from the dependence of F, Eq. (2.2), on ΔE (or ΔG). The quantum nature of the intramolecular vibrational modes is usually prevalent at all the relevant temperatures, as $k_B T \ll \hbar\omega_c$. When the medium modes can be handled in terms of the high temperature limit ($k_B T > \hbar\omega_m$), Eq. (2.2) reduces to[10]

$$F = (4\pi\lambda_m k_B T)^{-1/2}\exp(-S_c)\sum_{n=0}^{\infty}\frac{S_c^n}{n!}\exp\left[-\frac{(\Delta E+\lambda_m+n\hbar\omega_c)^2}{4\lambda_m k_B T}\right] \tag{2.7}$$

providing a useful contribution for the calculation of nuclear contributions to the ET rate over a broad temperature domain. In the limit $S_c = 0$, Eq. (2.7) reduces to the classical Marcus relation,[2] $F_{cl}(S_c{=}0) = (4\pi\lambda_m k_B T)^{-1/2}\exp[-(\Delta E+\lambda_m)^2/4\lambda_m k_B T]$ with a Gaussian activation energy. The (free) energy dependence of F (Fig. 3) provides a demonstration of the classical Marcus relation[2] in the normal region ($-\Delta E \le \lambda_m$) and in the activationless domain ($\Delta E = -\lambda_m$), while in the inverted region ($-\Delta E \ge \lambda_m$) marked deviations from the classical relation are exhibited (i.e., $F > F(S_c{=}0)$) due to the vibrational excitation of the quantum modes of D and A, accompanying ET. Quantum effects in the inverted region manifest a marked enhancement of the ET rate at constant ΔG (Fig. 3) and in a surprisingly weak temperature dependence of k for strongly exoergic reactions.[13]

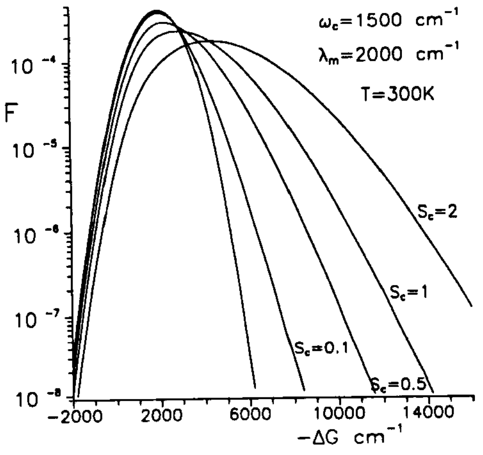

FIGURE 3 The energy gap dependence of the nuclear Franck-Condon factor.

Optimizing F Activationless ET

As is apparent from Fig. 3 the F factor is maximized ($F = F_{MAX}$) for $-\Delta E = \lambda_m + n\hbar\omega_c$, with the dominating contribution to the sum in Eq. (2.7) originating from the nth term, so that $F_{MAX} \simeq (4\pi\lambda_m k_B T)^{-1/2}(S_c^n/n!)\exp(-S_c)$. This situation corresponds to activationless ET, (i.e., for the lowest intersection of the multidimensional nuclear potential surfaces occurring at the minimum of the initial DA state) with a weak temperature dependent $k \propto T^{-1/2}$ non-Arrhenius-type rate. For typical values of $S_c \simeq 1$ the activationless ET is realized with $F_{MAX} \simeq (4\pi\lambda_m k_B T)^{-1/2} \exp(-S_c)$. The maximization of the Franck-Condon factor involves the optimization of the nuclear contribution to the ET rate.

In the nonadiabatic limit the optimal activationless rate is $k = (2\pi V^2/\hbar)F_{MAX}$. For characteristic values $\lambda_m = 4000$ cm^{-1} for ET in polar solvents or $\lambda \simeq 1000$ cm^{-1} in protein RC together with $S_c \simeq 1$, we estimate (at room temperature) the activationless ET rate

$$(k/\mathrm{sec}^{-1}) \simeq (1.4\text{-}2.7) \times 10^8 (V/\mathrm{cm}^{-1})^2 \quad . \tag{2.8}$$

For typical V values (Fig. 2) we estimate $k \simeq 2\mathrm{x}10^{10}$ sec^{-1} for $V = 10$ cm^{-1} and $V \simeq 2\mathrm{x}10^{12}$ sec^{-1} for $V \simeq 100$ cm^{-1}. The upper limit of the maximized activationless ET rate is determined by the breakdown of the nonadiabatic formalism, which requires the extension of the nonadiabatic theory.

3. EXTENSIONS OF CONVENTIONAL ET THEORY

Adiabatic ET

In section 2 we have spelled out the conditions for the applicability of the nonadiabatic ET theory. Condition (C) for weak electronic coupling, formulated within the framework of the theory of radiationless transitions, implies that the widths of the resonances (i.e., the decay rates k_i of individual initial states) are smaller than their separations (determined by an effective medium vibrational frequency $\omega_0 \sim \omega_m$) i.e., $\gamma = k_i/\omega_m < 1$. The coupling parameter is $\gamma = 2V^2/\hbar\omega_m(\lambda_m \hbar\omega_m)^{1/2} < 1$, which is similar to the Landau-Zenner parameter. Taking characteristic values of $\hbar\omega_m = 100$ cm^{-1} both for a protein medium and a polar solvent, nonadiabatic ET prevails for $V \lesssim 200$ cm^{-1} in a polar solvent ($\lambda_m \simeq 4000$ cm^{-1}) and $V \lesssim 100$ cm^{-1} for a protein medium ($\lambda_m \simeq 1000$ cm^{-1}). In Fig. 4 we have marked the upper limit for the V values, which still correspond to nonadiabatic ET. When the electronic coupling is sufficiently strong, i.e., $\gamma > 1$, the adiabatic limit for ET applies. The ET rate is then given by the Holstein formula $k = (\omega_m/2\pi)\exp(-E_a/k_B T)$. For activationless ET the adiabatic ET is $k \approx \omega_m/2\pi$.

Solvent-Controlled ET

The breakdown of assumption (D) in section 2 implies that solvent relaxation, rather than the microscopic electronic processes, constitutes the rate determining step for ET. For ET in a system solely characterized by coupling to the medium ($S_c = 0$), which corresponds to the normal Marcus region ($\Delta E \geq -\lambda_m$), the realization of solvent-controlled ET is determined by the magnitude of the solvent adiabaticity parameter[9] $\kappa = 4\pi V^2 \langle\tau\rangle / \hbar\lambda_m$, where $\langle\tau\rangle$ is the medium relaxation time induced by a constant charge distribution. In polar solvents $\langle\tau\rangle$ is the longitudinal dielectric relaxation time τ_L, e.g., τ_L = 200 fsec for water, τ_L = 190 fsec for acetonitrile and τ_L = 1.2 psec for methyl acetate.[9] For protein medium of the RC, molecular dynamics simulations give[14,15] $\langle\tau\rangle$ = 100 fsec over the temperature domain 10K-300K. The medium controlled ET rate is given by $k = k^{NA}/(1+\kappa)$, where the nonadiabatic rate k^{NA} is given by (2.1). In the limit $\kappa > 1$ $k \propto k^{NA}/\kappa \propto \langle\tau\rangle^{-1}$, being independent of V (Fig. 4).

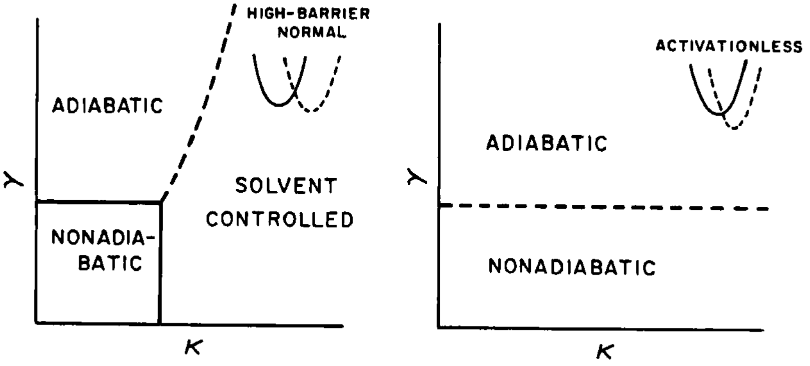

FIGURE 4 Domains for ET for the normal limit and for the activationless case.

Is this formalism relevant for activationless ET? Medium controlled ET will be manifested only provided that the microscopic rates are sensitive to the details of the distribution of the initial states. For activationless ET both model calculations in the classical limit and numerical computations reveal that the microscopic ET rates k_i are quite insensitive to the initial vibrational state.[11] This weak excess energy dependence of k_i is compatible with the weak temperature dependence of activationless ET. Accordingly, activationless ET is invariant with respect to medium relaxation dynamics, with the rate being independent of κ (Fig. 4). This analysis provides a possible explanation for the recent experimental observations of some ET rates, which substantially exceed the τ_L^{-1} limit predicted for solvent-controlled ET. Kobayashi et al.[16] reported ultrafast ET rates in (Nile bule$^+$)(TMPD) with $k \simeq (100\ \text{fsec})^{-1}$ which correspond to $k \simeq 50/\tau_L$, while Heitele et al.[17] observed for ET in porphyrin-quionone cyclophanes the independence of $k \approx (1\ \text{psec})^{-1}$ on κ (= 0.1-400) over a broad region. ET in both systems seems to correspond to activationless ET. The primary ET reactions in the photosynthetic RC are nearly activationless[13,14] whereupon the medium dynamics (with $\langle\tau\rangle \simeq 100$ fsec)[15] does not manifest explicitly in the rates. Thus activationless ET can be appreciably faster than previously expected, and is not limited by solvent dynamics.

An Upper Limit for Activationless ET

For activationless ET the nonadiabatic limit is expected to prevail, being characterized by $k \propto V^2$ with increasing V, until the adiabatic limit for ET will be achieved constituting an upper limit for the rate. An approximate estimate for the upper limit for the activationless ET rate can be inferred from Eq. (2.8) which, for a typical value of $\omega_m \simeq 100\ cm^{-1}$, results in $k^{-1} \gtrsim 300$ fsec. The fastest room temperature ET rates recorded up to date in synthetic supermolecules[16,17] and in the RC[18,19] (Table I) are either low or comparable to the theoretical upper limit.

TABLE I Some Ultrafast Activationless ET Lifetimes $\tau_{ET} = k^{-1}$ (T = 300K)

System	τ_{ET} (fsec)	Reference
Upper limit theoretical estimate	> 300	present work
(Nile Blue$^+$)TMPD in TMPD	100	16
porphirine-quionone paracyclophane in polar solvents	1000-2000	17
RC of *Rb.sphaeroides*		
$^1P^*BH \rightarrow P^+B^-H$	2600-3500	18,19
$P^+B^-H \rightarrow P^+BH^-$	1100± 400	
RC of *R.viridis*		
$^1P^*BH \rightarrow P^+B^-H$	3500± 400	20
$P^+B^-H \rightarrow P^+BH^-$	650± 200	

4. THE MOLECULAR LIMIT FOR ET

It has been dogmatic that long-range ET requires the coupling of the electronic states to the nuclear motion of the medium. The standard theory, i.e., $k \propto V^2F$ with F being given by Eq. (2.7) results in $k \rightarrow 0$ for $\lambda_m \rightarrow 0$ (for $n\hbar\omega_c \neq -\Delta E$), in accord with conventional "isolated" solvent-free supermolecules? This novel problem was addressed[8] by considering the vibrational coupling spectrum of a DBA system

$$C(\omega) = \sum_i (\Delta_i^2/2)\, \delta(\omega-\omega_i)\ , \tag{4.1}$$

which corresponds to the zero-temperature Fourier transform of $G_+(t)$, Eq. (2.4). $C(\omega)$ contains three contributions: (1) The medium modes, (2) medium-frequency intramolecular modes, and (3) high-frequency intramolecular modes. Contributions (1) + (3) to F were considered in section 2. The cumulative contribution of the intramolecular modes (2) + (3) may result in an intramolecular ET $D^*BA \rightarrow D^+BA^-$ in an "isolated" supermolecule. This molecular limit for ET, which constitutes an intramolecular electronic → vibrational radiationless transition, is analogous to internal conversion and intersystem crossing in "isolated" molecules.[1] The conditions for the realization of the molecular limit for ET are:

(1) An appropriate electronic level structure, with the charge transfer state constituting the lowest spin-allowed electronic excitation. The energetic condition for an appropriate electronic level structure is $R_{DA} \leq e^2/[I(D)-E(A)-E_0]$ where R_{DA} is the D-A (center-to-center) separation, E_0 the electronic excitation energy of D, I(D) the ionization potential of D and E(A) the electron affinity of A. For favorable energetics $R_{DA} \leq 7$Å, limiting the distance scale for charge separation in an isolated supermolecule.

(2) A sufficiently strong electronic coupling V between $S_2(M)$ and $S_1(CT)$. Electronic coupling via molecular bridges is sufficiently strong (Fig. 2) to warrant efficient V. In addition, substantial vibrational overlap integrals $\langle f_j \rangle$ between the neutral $S_2(M)$ state and the jth state of the charge transfer $S_1(CT)$ manifold (Fig. 5) are required.

(3) A large density ρ_j of background $S_1(CT)$ states, i.e., $2\pi(V\langle f_j\rangle\rho_j)^2 >> 1$. This situation will be realized for a sufficiently large energy gap between the electronic origins of $S_2(M)$ and $S_1(CT)$ (Fig. 5).

Under these circumstances the nonradiative decay rate of a single vibronic level of $S_2(M)$ is $k = (2\pi/\hbar)\, V^2\, \langle f_j \rangle^2 \rho_j$. The experimental implications of molecular ET induced by optical excitation to $S_2(M)$ are:

(1) Ultrafast (psec) decay of $S_2(M)$.

(2) Line broadening of the $S_2(M)$ manifold.

(3) Sequential molecular ET $S_2(M) \rightarrow S_1(CT) \rightarrow S_0(M)$.

(4) Small solvent effects on $S_2(M)$-$S_1(CT)$ and on $S_1(CT)$-$S_0(M)$ coupling and relaxation.

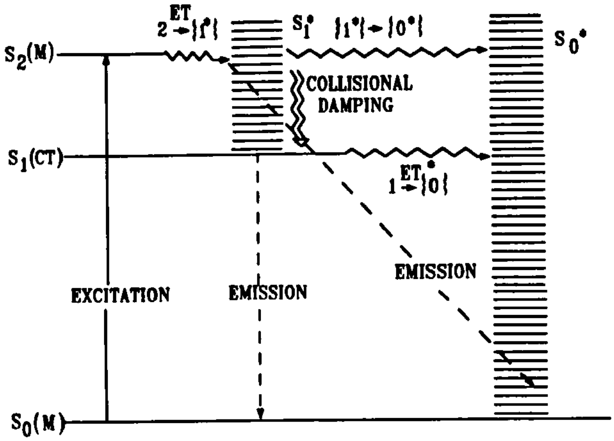

FIGURE 5 The molecular limit of ET in an isolated supermolecule as an intramolecular radiationless transition. Optical $S_0(M) \rightarrow S_2(M)$ excitation (vertical arrow ↑) initially selects a vibronic $S_2(M)$ level. This $S_2(M)$ state undergoes a radiationless transition to the $\{S_1^*\}$ manifold quasidegenerate with it (denoted $2 \rightarrow \{1^*\}$). Subsequently, the $\{S_1^*\}$ manifold undergoes a radiationless transition to the S_0^* manifold in the same energy domain (denoted $\{0^*\}$). Collisional damping by gas collisions or in solution (double vertical arrow) can bring the S_1 manifold to the vicinity of its electronic origin. Radiative decay competes with $S_1 \rightarrow \{S_0\}$ nonradiative decay.

(5) Excess vibrational energy dependence of the ET rate in "isolated" molecules, which is expected to be weak for the $S_2(M)$ manifold and pronounced for the $S_1(CT)$ states.

(6) Energy gap dependence. The ET rate for the $S_1(CT) \rightarrow S_0(M)$ radiationless decay from the electronic origin of $S_1(CT)$, which is reached by collisional damping (Fig. 5), is expected to exhibit an exponential energy gap (ΔE) law $k \simeq A \exp(-\gamma \Delta E/\hbar\omega_M)$, where ω_M is a high frequency intramolecular vibrational frequency and $\gamma \simeq 1\text{-}2$. The exponential relation for an "isolated" molecule replaces the Gaussian relation for conventional ET.

We now enquire what the situation is on the experimental front. Intramolecular photoinduced excimer formation and intermolecular exciplex formation were observed under solvent-free conditions.[21-23] This situation pertains to ET between D and A in close contact. Indirect information which points towards the dominance of the molecular limit in some supermolecules involves the possible applicability of the exponential energy gap law,[24] for a series of exciplexes in solution. Up to now long-range ET in an isolated supermolecule was not yet experimentally observed.

The molecular limit for ET establishes the analogy between intramolecular ET and intramolecular radiationless transitions. The ideological basis for the occurrence of molecular ET rests on the formal analogy between the contributions of the medium and intramolecular modes to the vibrational coupling spectrum, Fig. (5). Thus in some supermolecules satisfying appropriate constraints, fast and efficient long-range molecular ET in "solvent free" systems is expected to occur. This analysis is of significance for the construction of molecular devices in the area of molecular electronics. Of course, a most efficient molecular switch, where photoinduced charge separation over a distance of ~35Å occurs within 200 psec, involves the photosynthetic RC.[7,14,18-20] Regarding the processes of ET within the RC and other biomolecules, all the contributions to the vibrational coupling spectrum from both the protein modes and the intramolecular modes of the prosthetic groups have to be incorporated, with their cumulative contributions resulting in the optimization of ET in biological systems.

ACKNOWLEDGMENT

This research was supported by a grant from the BMFT (Contract No. 317-4003-0328955A) under the auspices of the University of Munich.

REFERENCES

1. J. Jortner and R.D. Levine, Adv. Chem. Phys., 47, 1 (1981).
2. R.A. Marcus and N. Sutin, Biochim. Biophys. Acta, 811, 265 (1985).
3. G.L. Closs, L.T. Calcaterra, N.J. Green, K.W. Penfield and J.R. Miller, J. Phys. Chem., 90, 3673 (1986).
4. C.A. Stein, N.A. Lewis and G.J. Seitz, J. Am. Chem. Soc., 104, 2596 (1982).
5. S.S. Isied, A. Vassilian, J.F. Wishart, C. Creutz, H.A. Schwarz and N. Sutin, J. Am. Chem. Soc., 109, 635 (1988).
6. K.W. Penfield, J.R. Miller, M.N. Paddon-Row, E. Cotsaris, A.M. Oliver and N.S. Hush, J. Am. Chem. Soc., 109, 5061 (1987).
7. J. Jortner and B. Pullman, editors, Perspectives in Photosynthesis (Kluwer Academic Publishers, Dordrecht, 1990).
8. J. Jortner, M. Bixon, H. Heitele and M.E. Michel-Beyerle, Chem. Phys. Lett. (in press).
9. I. Rips and J. Jortner, J. Chem. Phys., 87, 6513 (1987).
10. J. Jortner, J. Chem. Phys., 64, 4860 (1976).
11. M. Bixon and J. Jortner (to be published).
12. P. Siddart and R.A. Marcus, J. Phys. Chem., 94, 2985 (1990).

13. M. Bixon and J. Jortner, J. Phys. Chem., 95, 1941 (1991).
14. M. Bixon, J. Jortner and M.E. Michel-Beyerle, Biophys. Biochim. Acta, 1056, 30 (1991); and to be published.
15. K. Schulten and M. Tesch, Chem. Phys., 158, 421 (1991).
16. T. Kobayashi, Y. Takagi, H. Kandori, K. Kemnits and K. Yoshihara, Chem. Phys. Lett., 180, 416 (1991).
17. H. Heitele, F. Pöllinger, K. Kremer, M.E. Michel-Beyerle, M. Futscher, G. Voit, J. Weiser and H. Staab, Chem. Phys. Lett. (in press).
18. W. Holzapfel, U. Finkele, W. Kaiser, D. Oesterhelt, H. Scheer, H.U. Stilz and W. Zinth, Proc. Natl. Acad. Sci. USA, 87, 5168 (1990).
19. C.K. Chan, T.J. DiMango, K.X.Q. Chen, J. Norris and G.R. Fleming, Proc. Natl. Acad. Sci. USA, 88, 11202 (1991).
20. K. Dressler, E. Umlauf, S. Schmidt, P. Hamm, W. Zinth, S. Buchanan and H. Michel, Chem. Phys. Lett., 183, 270 (1991).
21. J.A. Syage, P.M. Felker and A.H. Zewail, J. Chem. Phys., 81, 2233 (1984).
22. B. Wegewijs, R.M. Hermant, J.W. Verhoeven, A.G.M. Kunst and R.P.H. Retteschnik, Chem. Phys. Lett., 140, 587 (1987).
23. A. Amirav, M. Castella, F. Piuzzi and A. Tramer, J. Phys. Chem., 92, 5500 (1988).
24. T.A. Sahi and N. Mataga, J. Phys. Chem., 95, 1956 (1991).